Dual Metal Synergistic Modulation of Boron Nitride for High-temperature Wave-Transparent Metamaterial

Zhangwen Xie[a], Yufei Tang[a]*, Ziyun Luo[a], Yagang Zhang[a], Wanxing Zheng[a], Xi Chen[a], Qingnan, Meng[a], Chen Tang[a], Zhaowei Liu[a], Kang Zhao[a]

a. School of Materials Science and Engineering, Shaanxi Province Key Laboratory of Corrosion and Protection, Xi'an, 710048, PR China

*Corresponding author

E-mail address: yftang@xaut.edu.cn

Characterization and performance measurements

The compositions of the prepared samples were investigated by X-ray photoelectron spectroscopy spectra (XPS, EscaLab 250) and Scanning electron microscope (SEM, JEM-6700F, Japan) linked to an energy-dispersive X-ray spectrometer (EDS), respectively. X-ray diffraction (XRD-7000S, Japan) patterns was used to phase analysis, with a working voltage of 40 kV, a working current of 200 mA, and a scanning speed of 8°/min. Scanning electron microscope (SEM, Merlin Compact, Germany) and Transmission electron microscope (TEM, JEM-3010, Japan) were used to investigate the morphologies and elements distribution. A Condenser Lens Spherical Aberration Correction Transmission Electron Microscope (JEM-ARM200CF NEOARM, Japan) was used to investigate the atomic structure. A contact angle tester (JGW-360B, China) was carried out to evaluate the hydrophobicity of all samples. Firstly, all powder samples were firstly prepared into films by using a spatula and leveler to ensure a smooth surface formed [1]. Then, a

deionized water droplet with a volume of 12 μL was generated by a syringe and gently dripped on the surface of the powder film when measuring the tangent angle at the contact point of the three phases [2, 3]. The vector network analyzer (VAN, PNA-N5244A, USA) was employed to measure the complex permittivity including the real part (ε′), imaginary part (ε″) at 2 to 18 GHz based on the coaxial flange method [4, 5]. The as-prepared specimens (19 mg) and paraffin (76 mg) were homogeneously mixed and pressed into mold to prepare coaxial ring with inner and outer diameters of 3.04 and 7.00 mm, respectively. High-temperature tube furnace (GSL-1700X, China) and thermogravimetric analysis (TGA, setaram-Setline, Franch) were carried out to evaluate the antioxidation performance of materials in air with a heating rate of 25 °C/min from 50 to 1500 °C.

The calculation of simulated electromagnetic wave transmittance

The simulated electromagnetic wave transmittance of materials was calculated based on S parameter according to Eq.S1-S3[6]. Firstly, the measured dielectric constant was imported in Computer Simulation Technology 2023 software and constructed a rectangular cavity model (length:10 mm, width: 10 mm, and height: 0.1-3.5 mm). The four side surfaces of the model were set as boundary conditions, while the two were configured as Floquet ports (Port1 and Port2). Subsequently, a frequency scanning range from 2 to 18 GHz with a step size of 0.02 GHz was set and the automatic calculation process was initiated. Finally, the transmittance can be obtained by the S-parameters.

$$S_{21} = 20\log\left|\frac{p_t}{p_i}\right| \qquad \textbf{Eq. S1}$$

$$T_{stimulation} = \left|\frac{p_t}{p_i}\right| \qquad \textbf{Eq. S2}$$

$$T_{simulation} = 10^{\frac{S_{21}}{20}} \qquad \textbf{Eq. S3}$$

Where, Pi denotes the power of electromagnetic waves transmitted from port 1, Pt represents the power received by port 2 after the electromagnetic wave has passed the material.

Table S1 The nominal compositions and their actual compositions measured by EDS for different Ca_x-Al_{1-x}-BN before and after oxidation

Sample	The total content of $CaCl_2•2H_2O$ and $AlCl_3•6H_2O$ (g)	The molar content of Ca and Al of Ca-Al mixture (mol)		Ca/(Ca+Al)[A]	Ca/(Ca+Al)[B]	Ca/(Ca+Al)[C] after oxidation measured by SEM-EDS		
		Ca	Al			at 1300℃	at 1400℃	at 1500℃
1Ca-0Al-BN	1.554	0.011	0	1.000	1	1	1	1
0.9Ca-0.1Al-BN	1.554	0.009	0.001	0.899	0.848	0.808	0.809	0.879
0.7Ca-0.3Al-BN	1.554	0.006	0.003	0.700	0.751	0.615	0.607	0.68
0.5Ca-0.5Al-BN	1.554	0.004	0.004	0.499	0.467	0.462	0.455	0.434
0.3Ca-0.7Al-BN	1.554	0.002	0.005	0.300	0.387	0.364	0.315	0.304

Ca/(Ca+Al)[A]: the mole proportion of Ca calculated by practical feeding ratio of $CaCl_2•6H_2O$ and $AlCl_3•6H_2O$ in Ca-Al mixture

Ca/(Ca+Al)[B]: the mole proportion of Ca calculated by SEM-EDS measurement

Ca/(Ca+Al)[C]: the mole proportion of Ca after oxidation calculated by SEM-EDS measurement

Samples	ε′(1)	tanδ	ε′(2)	Maximum operating temperature	Frequency	Refs.
Slip Cast Fused Silica	3.17	2×10^{-4}	3.42	1371℃	10 GHz	7
Al_2O_3	9.3	1×10^{-4}	10.3	1093℃	10 GHz	8
Si_3N_4w/SiO_2	3.37	1.1×10^{-2}	/	1270℃	10 GHz	9
$Si_3N_{4f}/BN/Si_3N_4$	About 5	About 0.04	4.7	1200℃	X-band	10
SiBCN	2.65-2.84	1.3×10^{-5}-1.6×10^{-2}	3.3	1400℃	X-band	11
Si_3N_4 hollow microsphere	2.60-2.90	5.06×10^{-2}-2.1×10^{-1}	/	1450℃	X-band	12
Ho_2SiO_5	6.6	8.3×10^{-3}	/	/	9.7 GHz	13
Li1Al1	About 2.8	0-6×10^{-2}	/	/	2-18 GHz	14
BN aerogel	1.03	1.6×10^{-2}	/	750℃	4-18 GHz	15
Si_3N_4 Aerogel	About 1.1	1.5×10^{-2}	1.23	1200℃	X-band	16
PEN/SiO_2 foams	1.71	4.7×10^{-3}	1.9	120℃	1 MHz	17
0.5Ca-0.5Al-BN	0.38-0.84	0.07-0.19	0.75-2.00	1500℃	2-18 GHz	This study

Table S2 The performance comparisons between 0.5Ca-0.5Al-BN and other wave-transmitting materials

ε′(1) represents the real part of dielectric constant at room temperature

ε′(2) represents the real part of dielectric constant at maximum operating temperature

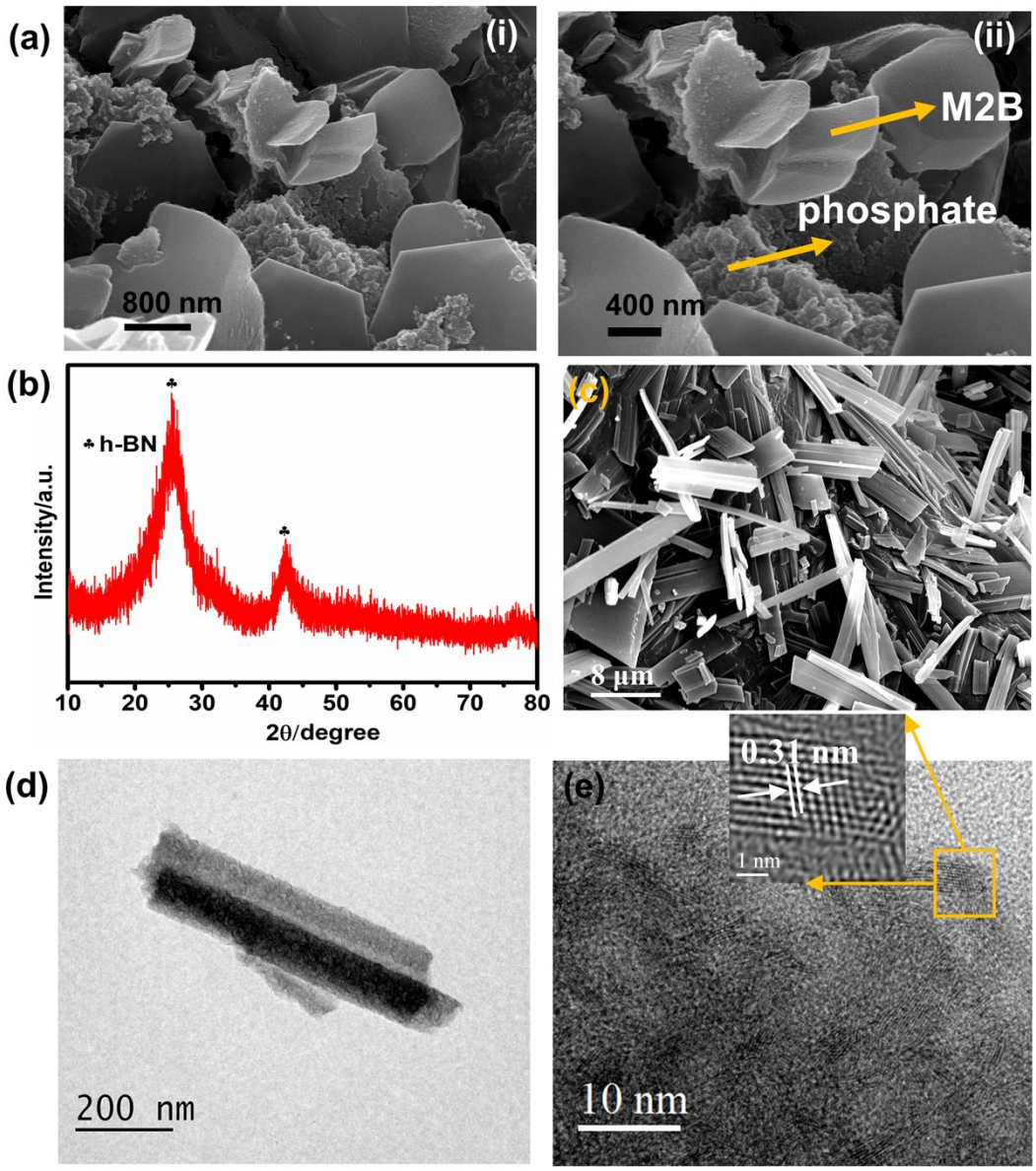

Fig.S1 (a-b) SEM images of Ca-Al phosphate doped M2B mixture, (b) XRD pattern, (c) SEM image, (d) TEM image and (e) HR-TEM images of h-BN

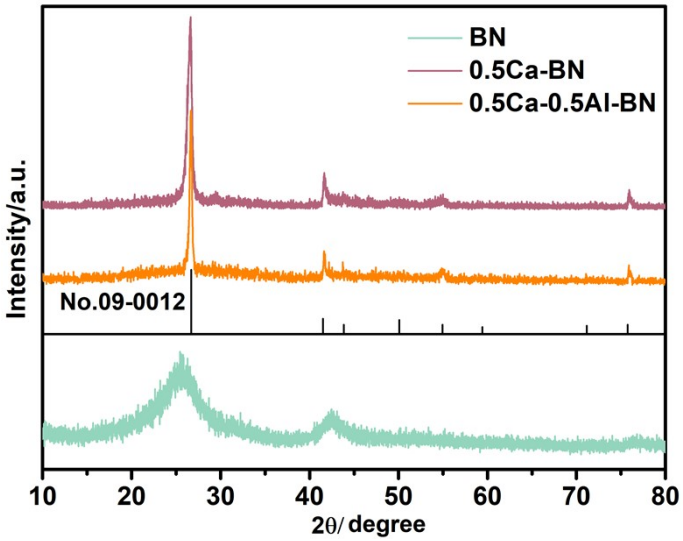

Fig.S2 XRD patterns of BN, 0.5Ca-BN and 0.5Ca-0.5Al-BN

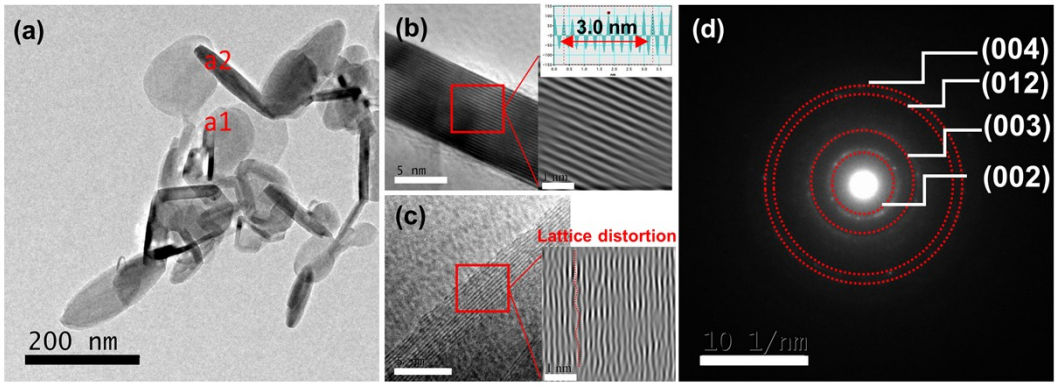

Fig.S3 (a) TEM and (b-c) HR-TEM images from a1 and a2 areas of (a), and (d) the corresponding SAED patterns of 0.5Ca-BN

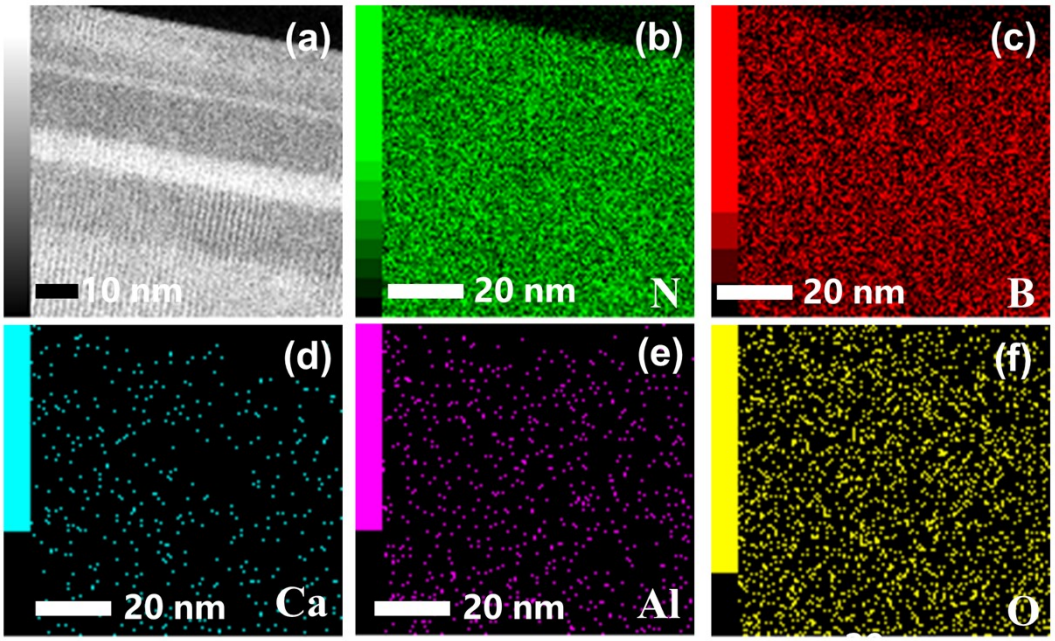

Fig.S4 HR-TEM image (a) and (b-f) the corresponding elements mapping of 0.5Ca-0.5Al-BN

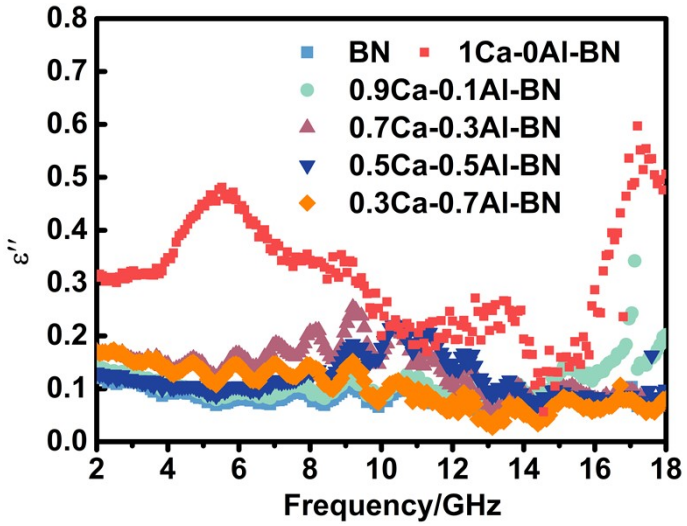

Fig. S5 The imaginary part of the complex permittivity of 0.5Ca-0.5Al-BN

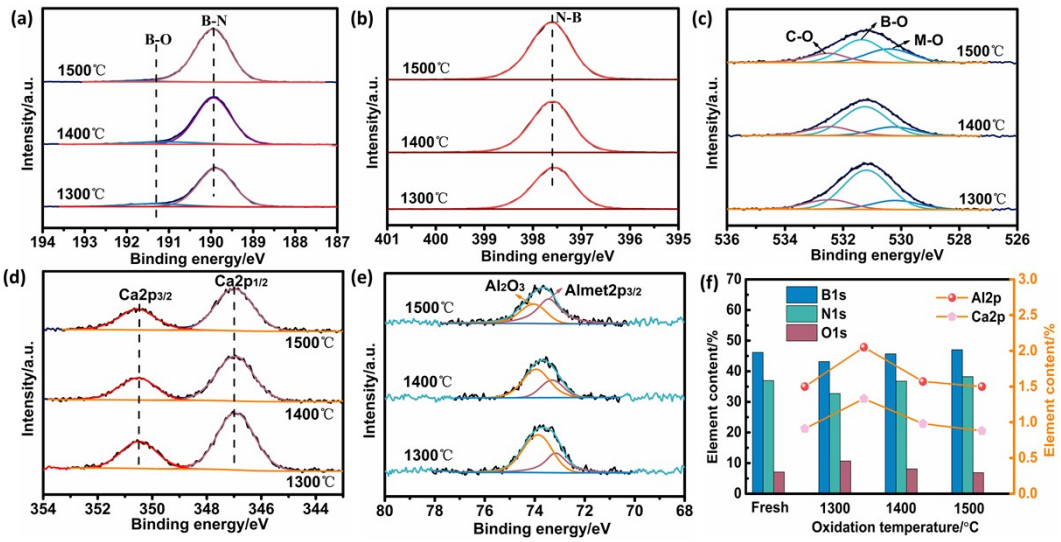

Fig.S6. XPS spectra of 0.5Ca-0.5Al-BN after oxidizing: (a) B1s, (b) N1s, (c) O1s, (d) Ca2p and (e) Al2p and (f) the atomic ratio of elements in 0.5Ca-0.5Al-BN before and after oxidation at different temperatures

References

1. D. La Zara, F. Zhang, F. Sun, M. R. Bailey, M. J. Quayle, G. Petersson, S. Folestad and J. R. van Ommen, Appl. Mater. Today, 2021, 22, 100945.
2. S. Wu, J. Fitzpatrick, K. Cronin, V. Maidannyk and S. Miao, J. Food Eng., 2020, 266, 109694.
3. J. Ji, J. Fitzpatrick, K. Cronin, P. Maguire, H. Zhang and S. Miao, Food Hydrocoll., 2016, 58, 194-203.
4. D. Li, D. Jia, Z. Yang and Y. Zhou, Int. Mater. Rev., 2022, 67, 266-297.
5. M. Qin, L. Zhang, X. Zhao and H. Wu, Adv. Sci., 2021, 8, 2004640.
6. Z. Liu, X. Fan, J. Zhang, L. Chen, Y. Tang, J. Kong and J. Gu, J MATER SCI TECHNOL, 2023, 152, 16-29.
7. T. Kenion, N. Yang and C. Xu, J. Eur. Ceram. Soc., 2022, 42, 1-17.
8. M. S. Heydari, J. Ghezavati, M. Abbasgholipour and B. M. Alasti, Sci. Iran., 2017, 24, 1136-1147.
9. M. Huang, Z. Peng, W. Zhang, Y. Xiang and F. Cao, Int. J. Appl. Ceram. Technol., 2022, 19, 2916-2924.
10. J. Zhou, L. Cheng, F. Ye, L. Zhang, Y. Liu, X. Cui and Z. Fu, J. Eur. Ceram. Soc., 2020, 40, 5305-5315.
11. Z. Yu, M. Ma, Z. Liu, Z. Zhang, C. Luo, T. Zhang and J. Kong, J MATER SCI TECHNOL, 2024, 196, 162-170.
12. K. Zhao, L. Cheng, F. Ye, S. Cheng and X. Cui, ACS Appl. Mater. Interfaces, 2019, 11, 39054-39061.
13. Y. H. Du, Z. L. Tian, L. Y, Zheng, Z.L. Chen, K.Y. Ming and B. Li, Ceram. Int., 2024, 50, 32187-32197.
14. L. Xia, Y. Yang, X. Zhang, J. Zhang, B. Zhong, T. Zhang, H. Wang and G. Wen, Ceram. Int., 2018, 44, 14896-14900.
15. J. Wang, L. Cheng, F. Ye and K. Zhao, ACS Appl. Mater. Interfaces, 2023, 15, 47405-47414.
16. C. Guo, F. Ye and L. Cheng, Compos. Part B Eng., 2021, 224, 109129.
17. Q. Qi, P. Zheng, Y. Lei and X. Liu, Compos. Part B Eng., 2019, 173, 106915.